Anal. Chem. **2006,** *78,* 6246−6251

Quantitative Intracellular Molecular Profiling Using a One-Dimensional Flow System

Leiji Zhou, Kemin Wang,* Weihong Tan, Yunqing Chen, Xinbing Zuo, Jianhui Wen, Bin Liu, Hongxing Tang, Lifang He, and Xiaohai Yang

Biomedical Engineering Center, State Key Lab of Chemo/Biosensing & Chemometrics, College of Chemistry & Chemical Engineering, College of Materials Science & Engineering, Hunan University. Engineering Reasearch Center for Bio-Nanotechnology of Hunan Province, Changsha 410082, China

We report on the development of one-dimensional microfluidic bead arrays for rapid and quantitative molecular profiling of human cancer cells. This new bioanalytical platform integrates the rapid binding kinetics of suspension bead carriers, the multiplexing and encoding capabilities of gene/protein chips, and the liquid handling advantages of microfluidic devices. Using antibody-conjugated beads in a two-site "sandwich" format, we demonstrate that the proteomic contents of as few as 56 human lung epithelial cancer cells can be determined with high sensitivity and specificity. The results indicate that each cell contains $\sim 6 \times 10^5$ copies of the tumor suppressor protein P53. We have further examined the expression changes of P53, c-Myc, and β-Actin as a function of anticancer drug treatment and have validated these changes by using Western blotting. This ability to quantitatively analyze normal and diseased cells raises new possibilities in studying cancer heterogeneity and circulating tumor cells.

We have developed a novel one-dimensional (1-D) flow system for rapid and quantitative molecular profiling of human cancer cells. It is based upon microbead arrays enclosed in bead-addressable microfluidic devices. Rapid and quantitative analysis of genes and proteins in living cells is important not only in basic molecular and cell biology but also in ultrasensitive medical diagnostics and biotechnology.[1−5] Recent advances in biochips, encoded beads, and microfluidic devices have allowed high-throughput analysis of genes and proteins in homogenized cellular samples;[6−10] however, these technologies do not allow routine chemical analysis at the level of individual cells, and each of them has its own advantages and limitations. As a result, sensitive single-cell studies are currently carried out using multicolor fluorescence imaging or cytometry, in which multiple molecular probes are used to recognize multicolor cellular targets.[11] In particular, the development of green fluorescent proteins has made a major impact in molecular and cell biology,[12,13] and a new generation of nanoparticle imaging probes could further expand the sensitivity and resolution of single-molecule and single-cell imaging.[14−16] However, it is difficult to design imaging-based methods to be quantitative due to problems with photobleaching, sampling, and data acquisition and processing. Here, we report the development of linear microbead arrays enclosed in periodic microfluidic devices for rapid and quantitative molecular profiling of human cancer cells. This new platform combines the multiplexing and encoding capabilities of gene/protein chips, the rapid binding kinetics of homogeneous assays, and the liquid handling functions of microfluidics.

Previous research[17,18] has developed bead-based fiber-optic arrays by randomly distributing DNA probes in chemically etched wells at the end of an imaging fiber bundle. This type of "random arrays" provides a high degree of flexibility because new probes can be readily added to detect new genes. In a different approach,[19] quantum-dot (QD)-encoded microbeads were developed by incorporating multicolor QDs into polymer beads at precisely controlled ratios. Similarly, fluorescent silica nanoparticles have been developed for multiplexing bioanalysis.[20] Each embedded with a spectroscopic signature or "bar code," these beads can be

* Corresponding author. E-mail: kmwang@hnu.cn.

(1) Irish, J. M.; Hovland, R.; Krutzik, P. O.; Perez, O. D.; Bruserud, O.; Gjertsen, B. T.; Nolan, G. P. *Cell* **2004**, *118*, 217−228.
(2) Wang, W.; Wyckoff, J. B.; Frohlich, V. C.; Oleynikov, Y.; Huttelmaier, S.; Zavadil, J.; Cermak, L.; Bottinger, E. P.; Singer, R. H.; White, J. G.; Segall, J. E.; Condeelis, J. S. *Cancer Res.* **2002**, *62*, 6278−6288.
(3) Levsky, J. M.; Shenoy, S. M.; Pezo, R. C.; Singer, R. H. *Science* **2002**, *297*, 836−840.
(4) Freeman, T. C.; Lee, K.; Richardson, P. J. *Curr. Opin. Biotechnol.* **1999**, *10*, 579−582.
(5) Horan, P. K.; Wheeless, L. L. *Science* **1977**, *198*, 149−157.
(6) Santini, J. T., Jr.; Cima, M. J.; Langer, R. A. *Nature* **1999**, *397*, 335−338.
(7) Service, R. F. *Science* **1998**, *282*, 396−399.
(8) Alper, J. *Science* **1990**, *247*, 804−806.
(9) Melton, L. *Nature* **2004**, *429*, 101−107.
(10) Verpoorte, E. *Lab Chip* **2003**, *3*, 60N−68N.
(11) Perfetto, S. P.; Chattopadhyay, P. K.; Roederer, M. *Nat. Rev. Immunol.* **2004**, *4*, 648−655.
(12) Tsien, R. Y. *Annu. Rev. Biochem.* **1998**, *67*, 509−544.
(13) Shaner, N. C.; Campbell, R. E.; Steinbach, P. A.; Giepmans, B. N.; Palmer, A. E.; Tsien, R. Y. *Nat. Biotechnol.* **2004**, *22*, 1567−1572.
(14) Gao, X.; Yang, L.; Petros, J. A.; Marshall, F. F.; Simons, J. W.; Nie, S. *Curr. Opin. Biotechnol.* **2005**, *16*, 63−72.
(15) Chan, W. C. W.; Maxwell, D. J.; Gao, X.; Bailey, R. E.; Han, M.; Nie, S. *Curr. Opin. Biotechnol.* **2002**, *13*, 40−46.
(16) Michalet, X.; Pinaud, F. F.; Bentolila, L. A.; Tsay, J. M.; Doose, S.; Li, J. J.; Sundaresan, G.; Wu, A. M.; Gambhir, S. S.; Weiss, S. *Science* **2005**, *307*, 538−544.
(17) Steemers, F. J.; Ferguson, J. A.; Walt, D. R. *Nat. Biotechnol.* **2000**, *18*, 91−94.
(18) Walt, D. R. *Science* **2000**, *287*, 451−452.
(19) Han, M. Y.; Gao, X. H.; Su, J. Z.; Nie, S. M. *Nat. Biotechnol.* **2001**, *19*, 631−635. Gao, X. H.; Nie, S. M. *Anal. Chem.* **2004**, *76*, 2406−2410.
(20) Wang, L.; Yang, C. J.; Tan, W. *Nano Lett.* **2005**, *5*, 37−43. Wang, L.; Tan W. *Nano Lett.* **2006**, *6*, 84−88.

10.1021/ac060598e CCC: $33.50
Published on Web 07/26/2006

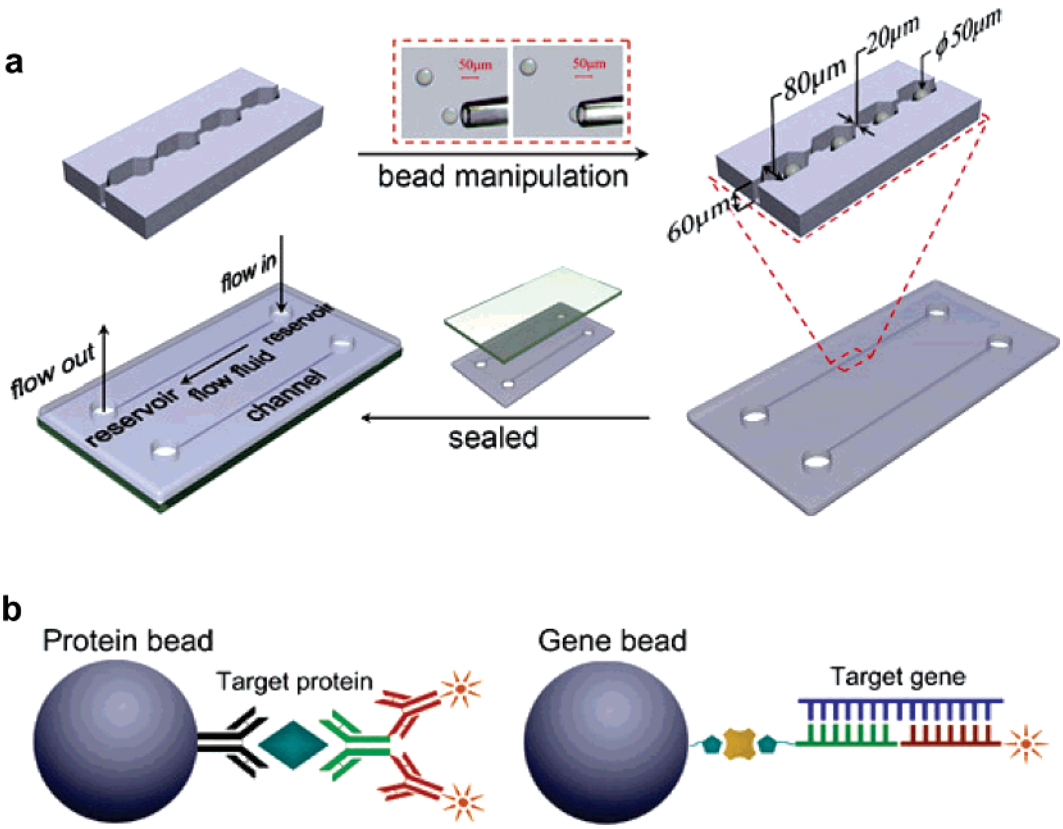

Figure 1. Schematic illustrations of microfluidic bead array assembly and bioconjugated beads for protein and gene detection. (a) Deposition of individual beads into enclosed chambers along a microfluidic channel, followed by channel sealing with a prefabricated top plate. Note that the relative dimensions of the bead, the channel, and the chambers allowed a single bead to be suspended in the chamber but not to flow through the interconnecting channel. (b) Structure and principle of two-site sandwich immunoassay and DNA hybridization for protein and nucleic acid detection. See text for detailed discussion.

used for simultaneous and multiplexed analysis of biomolecules in solution. These encoded beads, however, have not been integrated with microfluidic devices and have achieved only limited success in practical applications.

In this work, we have fabricated linear bead arrays by depositing individual beads in periodic chambers along a microfluidic flow channel. Each of the microfabricated chambers holds a single bead, with interconnecting channels for liquid flow. The bead is suspended and is free to move within its enclosing chamber, but it cannot move through the narrow connection channels. When sealed with a top plate, these linear bead arrays are engineered into simple and inexpensive devices that are well-suited for quantitative biomolecular analysis. Using a two-site "sandwich" immunoassay format, we have measured the average number of P53 molecules in single cancer cell and have examined drug-induced expression changes of three proteins (P53, c-Myc, and β-Actin) in cultured cancer cells. These results highlight new opportunities in understanding the complex molecular events that drive cancer development and progression and in ultrasensitive detection of protein biomarkers in cellular lysates.

EXPERIMENTAL SECTION

Bead Preparation and Bioconjugation. Mouse anti-P53 and mouse anti-β-Actin monoclonal antibodies were purchased from Wuhan Boster Bio. Tech. Ltd. Mouse monoclonal anti-c-Myc was provided by Zymed Laboratories, Inc. These antibodies were ultrafiltered with centrifugal filter units (Microncon YM-100, Millipore) to remove the protective protein BSA before use. About 10 mg of silica beads (H4267, Sigma-Aldrich, St Louis, MO) was activated in a 0.5-mL tube by suspending them in 200 μL of 2 M Na_2CO_3 solution for 15 min. The activating agent, CNBr (0.1 g) in 100 μL of acetonitrile, was then added to and reacted together with the silica beads for 30 min. After reaction, the silica beads were washed three times thoroughly with ice water and 10 mM PBS at pH 7.4. The CNBr-activated beads were then suspended in 200 μL of 10 mM PBS (pH 7.4) containing 0.4 μg of mouse monoclonal antibody and were incubated for 24 h in a low-temperature shaker (4 °C, >300 rpm). The modified beads, after being washed three times with 10 mM PBS, were mixed with 200 μL of 0.3% BSA in 10 mM PBS containing 0.02% NaN_3 and were incubated for 12 h in a low-temperature shaker (4 °C, >300 rpm). After the modification, the surface-funtionalized beads were stored at 4 °C. Control beads were prepared with BSA using the same procedure.

Chip Fabrication and Assembly. Patterned silica masters were fabricated by Research Institute of Micro/Nano Science and Technology, Shanghai Jiao Tong University. For polymer molding on the patterned silica masters, a 10:1 mixture of PDMS prepolymer and the curing agent (Dow Corning Corporation Midland, MI) were stirred thoroughly and then degassed under vacuum. The polymer mixture was poured onto the master and cured for ~40 min at 75 °C. After curing, the PDMS replica was peeled from the master, and the wells were punched to define the

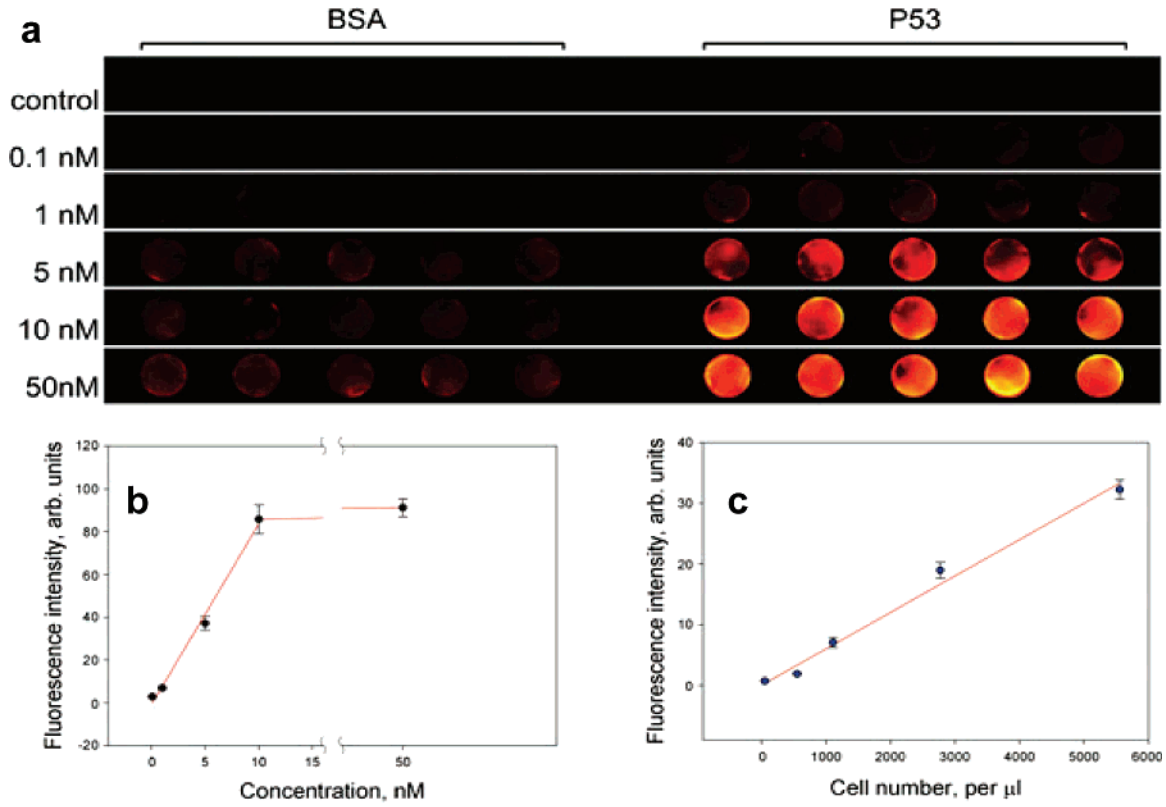

Figure 2. Quantitative protein detection using linear microfluidic bead arrays. (a) Fluorescence images of 5-fold redundant bead arrays for protein P53, together with BSA-coated beads for comparison. For top to bottom, the range of P53 concentrations were between 0 (control) and 50 nM. (b) Calibration plot of fluorescence intensity vs P53 concentration, showing a linear relationship between 0 and 10 nM target and signal saturation at higher concentrations. (c) Cancer cell lysate data obtained from cultured A549 cells at different cell concentrations (number of cells per microliter of lysate). The curve showed an excellent linear response between 0 and 6000 cells in each microliter.

reservoirs. The inner channel walls were coated with 5% polymethobromide (PB, Sigma-Aldrich Co.) and 3% dextran sulfate (DS, Tianjin H & Y Bio Co. Ltd.) solution.[21] Manipulation of the microbeads was performed by moving mouse monoclonal antibody-coated beads and BSA-coated blank beads into the microchambers one-by-one using the vacuum tweezers (Nikon Narishige, model NT88NEN, Nikon Corp., Japan) under the microscope (Leica DM IRB, Leica Corp., Germany). After the manipulation, the PDMS replica and a cleaned slide were placed in a plasma cleaner (PDC-002, Harrick Scientific Corp., Ossining, NY) and oxidized at high power for 1 min. Immediately after removal from the plasma cleaner, the substrates were brought into conformal contact, and an irreversible seal formed spontaneously.

On-Chip Detection. Total proteins from cultured cells were extracted by first precooling the cell culture bottle and washing it twice with 0.01 M PBS. Cell lysis buffer (0.15 M NaCl; 1.0% Triton X-100; 50 mM Tris−Cl, pH 8.0; 1.5 mM EDTA, pH 8.0) was stored at 4 °C, and 1 mM PMSF, 1 μM pepstatin A, and 10 μM leupeptin were added to the buffer before use. For on-chip protein detection, 2 μL of the cellular protein lysate was added into a reservoir and was loaded into the microchannel by gravity. After mixing with the beads for 20 min, the lysate in the reservoir was replaced with a washing buffer (0.15 M PBS, pH 7.4; 0.05% Tween-20; 0.02% NaN_3), and the channel and beads were washed for another 20 min. In subsequent steps, 2 μL of dilution of the rabbit polyclonal antibody, washing buffer, 2 μL of dilution of Cy3-labeled goat anti-rabbit IgG, and additional washing buffer were individually added in turn into the reservoir, followed by 20 min of flow through the microchannel by gravity. For the control experiment, new microfluidic bead array chips were used under the same conditions. Fluorescence imaging of the beads was achieved with a fluorescence microscope (Leica DM IRB, Leica Corp., Germany) equipped with a CCD camera (Leica DC 300F). aAnalysis was performed with microscope analysis software.

RESULTS AND DISCUSSION

Fabrication and Principles of Chip Operation. Figure 1a shows the process of assembling beads and microfluidic channels into linear bead arrays. Microfluidic flow channels (20 μm wide × 60 μm deep) were specially fabricated to contain periodic chambers (80 μm wide × 60 μm deep). On this open chip, vacuum tweezers were used to fill each chamber with a single bead (50-μm diameter). The chip was then sealed using a top plate with predesigned liquid outlets and reservoirs. Each chamber was large enough to hold a bead, but the interconnecting channel was too small for the bead to flow through. Thus, liquid could continuously flow through the channel, but the beads were confined in their original chambers. A major advantage of this "hybrid" design is that it allows both positional encoding by the chamber (similar to a spot in a gene microarray) and fast binding kinetics.[22,23]

(21) Katayama, H.; Ishihama, Y.; Asakawa, N. *Anal. Chem.* **1998**, *70*, 5272−5277.

(22) Nolan, J. P.; Mandy, F. F. *Cell. Mol. Biol. (Noisy-le-grand)* **2001**, *47*, 1241−1256.

Figure 1b illustrates the principles of bead functionalization, target binding, and fluorescence detection. Protein beads were developed by using capture antibodies that recognize and enrich a specific protein on the bead surface. The enriched target was recognized and selected by a secondary antibody and was then detected by using fluorescently tagged antibodies. Similarly, we developed gene beads by conjugating to capture DNA probes through a biotin−avidin linkage. These probes captured and enriched the target DNA, and fluorescence detection was achieved by using another DNA probe that was tagged with a fluorescent dye and was complementary to part of the target sequence. This "sandwich" type of protein immunoassay and DNA hybridization relies on a "double-selection" process to improve both detection sensitivity and specificity. In fact, a number of powerful diagnostic technologies are based on this sandwich format, such as latex agglutination tests,[24] enzyme-linked immunoabsorbent assays,[25] luminescent oxygen channeling immunoassay,[26,27] and fluorescence cross-correlation spectroscopy.[28,29] In this format, the target molecules do not need to be tagged or modified, but the excess probes must be washed away or otherwise differentiated from the bound targets. It is important to note that more than 160 chambers could be arranged along a 2-cm-long channel, with a total volume of <0.1 μL. Even with a 5-fold redundancy (that is, five identical beads are used to measure each target), our linear microfluidic arrays would allow more than 30 genes or proteins to be analyzed in samples as small as 0.1 μL.

Analysis of P53 in Single Cancer Cells. To evaluate detection sensitivity, dynamic range, and reproducibility, we prepared 5-fold redundant linear bead arrays for P53, one of the best-known tumor suppressors.[30] When it functions properly, P53 prevents uncontrolled growth of cells, a defining feature of cancer cells. In response to cellular stress, such as DNA damage, P53 is transported from the cytoplasm to the nucleus, where it transcriptionally activates genes that are involved in growth arrest and apoptosis.[31,32] In almost 50% of all human cancers, P53 is deactivated because of acquired mutations. Figure 2 (top) shows the fluorescence images of the bead arrays at various P53 concentrations, together with BSA-coated beads (also 5-fold redundancy) for comparison. A surprising result is that the fluorescence signals are not evenly distributed within a single bead, most likely due to defects or heterogeneities on the bead surface. However, the overall (integrated) intensities correspond linearly with P53 concentration, as judged by the small error bars (Figure 2, lower left). On the basis of a signal-to-noise ratio of 3, the achieved detection limit is ~0.05 nM, with a saturation concentration of 10 nM, giving rise to a linear dynamic range of 200. At higher P53 concentrations (5−50 nM), significant fluorescence background was observed, but these signals were reproducible and could be subtracted nearly completely.

On the basis of these calibration and lysate dilution studies, we have further determined the average copy number of intracellular P53 molecules in single lung cancer cells. For this purpose, we extracted 120 μL of cell lysate from 0.67 million A549 cells (corresponding to 56 000 cells/μL). For a series of diluted samples, the P53 fluorescence intensities were measured, and the limit of detection was calculated to be 56 cells per μL. To apply the "standard addition method", we measured the fluorescence intensity of a cell lysate sample (~1000 cells per μL), as well as the fluorescence intensity when this sample was mixed with an internal standard of 5 nM pure P53. The fluorescence intensity was found to increase from 6.7 to 35.6 (arbitrary units, canceled when these two values were ratioed during calculation) upon the addition of the P53 internal standard. From the simple equation

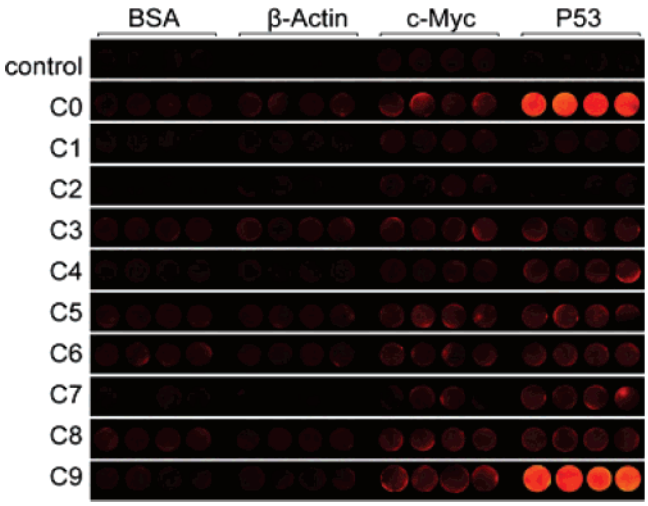

Figure 3. Fluorescence images of bead arrays detecting three cellular proteins (P53, beta-Actin, and c-Myc) in four cell lines (A549, HBE, CHO-p53, and CNE2) under different drug treatment conditions, together with BSA-coated beads for background subtraction. Control: background fluorescence in the absence of cell lysate. C0: untreated HBE cell. C1−C3: CHO-p53 cells treated with 5-FU for 0, 12, and 18 h, respectively. C4−C6: CNE2 cells treated with 5-FU for 0, 12, and 18 h, respectively. C7−C9: A549 cells treated with 5-FU for 0, 12, and 18 h, respectively.

Table 1. Two-Dimensional Matrix for Calculating Protein Concentrations in Various Cell Lines and under Different Drug Treatment Conditions

	BSA blank	β-Actin	c-Myc	P53
1. control	$F_{1,1}$	$F_{1,2}$	$F_{1,3}$	$F_{1,4}$
2. HBE	$F_{2,1}$	$F_{2,2}$	$F_{2,3}$	$F_{2,4}$
3. CHO-p53	$F_{3,1}$	$F_{3,2}$	$F_{3,3}$	$F_{3,4}$
4. CHO-p53 (5-Fu for 12 h)	$F_{4,1}$	$F_{4,2}$	$F_{4,3}$	$F_{4,4}$
5. CHO-p53 (5-Fu for 18 h)	$F_{5,1}$	$F_{5,2}$	$F_{5,3}$	$F_{5,4}$
6. CNE2	$F_{6,1}$	$F_{6,2}$	$F_{6,3}$	$F_{6,4}$
7. CNE2 (5-Fu for 12 h)	$F_{7,1}$	$F_{7,2}$	$F_{7,3}$	$F_{7,4}$
8. CNE2 (5-Fu for 18 h)	$F_{8,1}$	$F_{8,2}$	$F_{8,3}$	$F_{8,4}$
9. A549	$F_{9,1}$	$F_{9,2}$	$F_{9,3}$	$F_{9,4}$
10. A549 (5-Fu for 12 h)	$F_{10,1}$	$F_{10,2}$	$F_{10,3}$	$F_{10,4}$
11. A549 (5-Fu for 18 h)	$F_{11,1}$	$F_{11,2}$	$F_{11,3}$	$F_{11,4}$

(23) Nolan, J. P.; Sklar, L. A. *Trends Biotechnol.* **2002**, *20*, 9−12.
(24) Newman, D. J.; Henneberry, H.; Price, C. P. *Ann. Clin. Biochem.* **1992**, *29*, 22−42.
(25) Diamandis, E. P.; Christopoulos, T. K. *Immunoassay*; Academic Press: San Diego, CA., 1996.
(26) Ullman, E. F.; Kirakossian, H.; Switchenko, A. C.; Ishkanian, J.; Ericson, M.; Wartchow, C. A.; Pirio, M.; Pease, J.; Irvin, B. R.; Singh, S.; Singh, R.; Patel, R.; Dafforn, A.; Davalian, D.; Skold, C.; Kurn, N.; Wagner, D. B. *Clin. Chem.* **1996**, *42*, 1518−1526.
(27) Ullman, E. F.; Kirakossian, H.; Singh, S.; Wu, Z. P.; Irvin, B. R.; Pease, J. S.; Switchenko, A. C.; Irvine, J. D.; Dafforn, A.; Skold, C. N.; Wagner, D. B. *Proc. Natl. Acad. Sci. U.S.A.* **1994**, *91*, 5426−5430.
(28) Schwille, P.; Meyer-Almes, F. J.; Rigler, R. *Biophys. J.* **1997**, *72*, 1878−1886.
(29) Rigler, R. *J. Biotechnol.* **1995**, *41*, 177−186.
(30) Vogelstein, B.; Lane, D.; Levine, A. J. *Nature* **2000**, *408*, 307−310.
(31) Vogelstein, B.; Kinzler, K. W. *Cell* **1992**, *70*, 523−526.
(32) Vousden, K. H. *Cell* **2000**, *103*, 691−694.

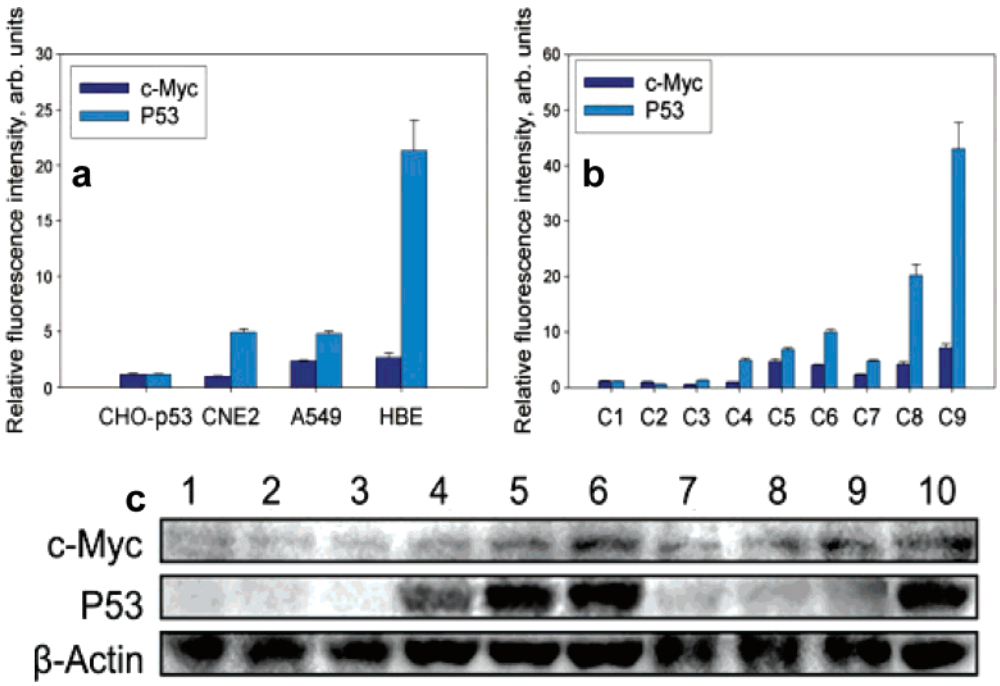

Figure 4. Quantitative comparisons of protein expression levels among different cell lines and under various drug treatment conditions. (a) Differences in P53 and c-Myc protein expression among four different cell liens (HBE, CHO−P53, CNE2 and A549). (b) Comparison of P53 and c-Myc expression in different cell lines under various drug treatment conditions. C1−C3: CHO-p53 cells treated with 5-FU for 0, 12, and 18 h. C4−C6: CNE2 cells treated with 5-FU for 0, 12, and 18 h. C7−C9: A549 cells treated with 5-FU for 0, 12, and 18 h. (c) Western blotting data for P53, c-Myc, and β-Actin. Lanes 1−3: CHO-p53 cells treated with drug for 0, 12, and 18 h. Lanes 4−6: A549 cells treated with drug for 0, 12, and 18 h. Lanes 7−9; CNE2 cells treated with drug for 0, 12, and 18 h; Lane 10: HBE cell without drug treatment.

of $6.7/C = 35.6/(C + 5)$, we found that the P53 concentration (nM), C, is equal to ~1.1 nM in the diluted lysate sample. Divided by the number of cells, one cancer cell yields a P53 concentration of .~1.0 pM in a 1.0-μL lysate solution. This corresponds to ~6×10^5 P53 intracellular molecules per A549 cell. Note that this value represents the average number of P53 molecules in single cancer cells and does not reveal the variations among cells. For direct chemical analysis of single cancer cells (that is, without using PCR or other amplification schemes), it will be necessary to reduce the cell lysate volume to 20 nL because our achieved sensitivity for P53 detection is ~50 pM.

Drug Effects on Cellular Protein Expression. Our linear microfluidic bead arrays provide a powerful platform for analyzing changes in cellular protein expression as a function of cancer drug treatment. Here, we demonstrate quantitative profiling studies of three cellular proteins (P53, c-Myc and β-Actin) in a number of cell lines after treatment with the anticancer drug 5-flouorouracil (5-FU). Proteins P53 and c-Myc are tumor-associated genes, and their expression products play important roles in cell growth, differentiation, and malignant transformation. β-Actin has a stable level of intracellular expression and is used as an internal control for P53 and c-Myc expression analysis. The selected cell lines were A549, human nasopharyngeal carcinoma cell line (CNE2), human bronchial epithelium cell line (HBE), and p53 gene-knockout Chinese hamster ovary cells (CHO-p53). To investigate drug-mediated differential protein profiling, the cultured cancer cells were exposed to 5-fluorouracil (10 μg/mL) for 0, 12, and 18 h. Four-fold redundant microfluidic bead arrays were constructed using mouse anti-P53 beads, mouse anti-c-Myc beads, mouse anti-β-Actin beads, and BSA-blocked control beads. Figure 3 shows the fluorescence images of bead arrays for three cellular proteins in three cell lines under different treatment conditions.

For quantitative data analysis, we used a two-dimensional matrix in which the relative signal intensities ($S_{i,\mathrm{P53}}$ and $S_{i,\mathrm{c-Myc}}$) for intracellular P53 and c-Myc proteins are derived according to these two equations,

$$S_{i,\mathrm{P53}} = \frac{(F_{i,4} - F_{i,1}) - (F_{1,4} - F_{1,1})}{(F_{i,2} - F_{i,1}) - (F_{1,2} - F_{1,1})} = \frac{\Delta S_{i,\mathrm{P53}}}{\Delta S_{i,\beta-\mathrm{Actin}}}$$

$$S_{i,\mathrm{c-Myc}} = \frac{(F_{i,3} - F_{i,1}) - (F_{1,3} - F_{1,1})}{(F_{i,2} - F_{i,1}) - (F_{1,2} - F_{1,1})} = \frac{\Delta S_{i,\mathrm{c-Myc}}}{\Delta S_{i,\beta-\mathrm{Actin}}}$$

where the subscript i is the row number of cell lines, ranging from 2 to 11. Table 1 shows the complete elements of this matrix.

In this matrix, elements $F_{i,1}$ are control BSA-bead values and provide a measure of nonspecific adsorption and binding on the beads; elements $F_{1,j}$ are background fluorescence signals and are observed in the absence of cell lystaes; and elements $F_{i,j}$ are bead signal values and are obtained for the jth protein in the ith cell line or treatment conditions. Quantitative protein results are shown in Figure 4, together with validation data obtained from standard Western blotting. In agreement with the p53 knockout nature of CHO-p53 cells, only residual P53 expression was observed in this cell line. In contrast, the HBE cell line exhibits a very high level of P53 expression. For the c-Myc protein, HBE and A549 cells have similar expression levels, whereas only low levels are observed in CNE2 and CHO-p53 cells. Upon 5-FU treatment for 12 and 18 h, both P53 and c-Myc expressions in A549 and CNE2 were upregulated, especially P53 in drug-treated A549 cells. For

CHO-p53 cells, however, P53 and c-Myc expressions were not sensitive to 5-FU treatment.

To validate the bead array protein data, we have carried out Western blotting on the same cell lysate samples. As shown in Figure 4c, the results confirmed that HBE has a higher P53 expression than A549 and CNE2 prior to drug treatment. After drug treatment, both P53 and c-Myc are significantly upregulated in A549 cells but not in CNE2 cells. For the p53 knockout CHO cells, both P53 and c-Myc have very low expression levels and were not responsive to drug treatment.

In conclusion, we have developed a 1-D flow system based on microbead arrays enclosed in bead-addressable microfluidic devices. These can be used for rapid and quantitative molecular profiling of human cancer cells. In comparison with current molecular profiling technologies, this "hybrid" platform combines the rapid binding kinetics of homogeneous assays, the multiplexing and encoding capabilities of protein chips, and the liquid handling advantages of microfluidic devices. Distinguished from the microwells, a major advantage of 1-D bead arrays is the low consumption of expensive reagents and valuable sample. The total volume of solutions flowing through all the chambers is as small as 0.1 μL. In addition, the analysis time is related to different reactions and is greatly saved in diffusion-controlled reaction systems under the flow situation. Using antibody-conjugated beads in a two-site "sandwich" immunoassay format, we have demonstrated that the proteomic contents of as few as 56 human lung epithelial cancer cells can be determined at picomolar target sensitivity. Using the standard addition method, we estimate that a single lung cancer cell contains $\sim 6 \times 10^5$ copies of the tumor suppressor protein p53. We have further examined the expression level changes of P53, c-Myc, and β-Actin as a function of anticancer drug treatment and have validated these changes by using standard Western blotting. This quantitative and multiplexed biochemical analysis of normal and diseased cells should facilitate new approaches to the fundamental study of cancer development and progression. It can also be used to provide more sensitive detection of the circulating tumor cells in blood/serum samples.

ACKNOWLEDGMENT

This work was supported in part by the Key Project of Natural Science Foundation of China (20135010), Key Project of International Technologies Collaboration Program of China (2003DF000039), and Key Technologies Research and Development Program of China (2003BA310A16). National Key Basic Research Program of China (2002CB513110), and Major International (Regional) Joint Research Program of Natural Science Foundation of China (20610107).

Received for review March 31, 2006. Accepted June 21, 2006.

AC060598E